Copper(II) Complexes with Anti-inflammatory Drugs as Ligands. Solution Behaviour and Electrochemistry of Mono- and Bi-nuclear Complexes†

Catherine Dendrinou-Samara,[a] Panagiotis D. Jannakoudakis,[b] Dimitris P. Kessissoglou,*[,a] George E. Manoussakis,[a] Dimitris Mentzafos[c] and Aris Terzis[c]

[a] *Laboratory of Inorganic Chemistry, Aristotle University of Thessaloniki, Thessaloniki 54006, Greece*
[b] *Laboratory of Physical Chemistry, Aristotle University of Thessaloniki, Thessaloniki 54006, Greece*
[c] *NRCPS 'Demokritos', Institute of Materials Science, 15310 Aghia Paraskevi Attikis, Greece*

The copper complexes of 1-methyl-5-(*p*-toluoyl)-1*H*-pyrrole-2-acetic acid (tolmetin, HL^1), α-methyl-4-(2-methylpropyl)benzeneacetic acid (ibuprofen, HL^2) and 6-methoxy-α-methylnaphthalene-2-acetic acid (naproxen, HL^3) common anti-inflammatory drugs, were prepared and characterized. The available evidence supports a dimeric structure for the dimethyl sulfoxide adducts, $[Cu_2L_4(dmso)_2]$, and monomeric for the pyridine (py) analogues, $[CuL(py)_2(H_2O)]$. The solution behaviour of the dimers in dimethylformamide (dmf) shows that the complexes are converted into monomeric compounds by addition of more than 25% of pyridine. The cyclic voltammograms of the dimers in dmf suggest that the complexes retain the dimeric structure in solution. The EPR spectra of the monomers as CH_2Cl_2–dmf (4:1) glasses confirm the monomeric structure, having a $d_{x^2-y^2}$ ground state. Paramagnetic ^1H NMR studies have shown that the H_2O molecule of the monomeric form remains co-ordinated to Cu^{II} in CD_3Cl, $(CD_3)_2CO$ or CD_3CN. The crystal structure of $[CuL^3_2(py)_2(H_2O)]$ has been determined: space group $P2_1$, a = 16.112(3), b = 5.8692(9), c = 18.130(3) Å, β = 75.818(7)°. In this complex the copper atom is five-co-ordinate. The atoms N(1) and N(2) of the two pyridine molecules and one carboxylate oxygen atom from each of the two ligands form the basal plane of a square pyramid with a water molecule at its apex.

It is well known that copper(II) complexes of inactive ligands and active anti-inflammatory drugs are more active than the ligands themselves.[1] Ligands such as anthranilic acid and 3,5-diisopropylsalicylic acid were found to be inactive, but their copper complexes were found to be anti-inflammatory agents.[2,3] Aspirin (2-acetyloxybenzoic acid) and D-penicillamine (3-mercapto-D-valine), active anti-inflammatory agents, were shown to be more effective as their copper complexes.

The most used anti-inflammatory drugs are carboxylic acids in which the carboxylate group is available for metal–ligand interaction.[4] Many binuclear copper(II) carboxylate compounds have been isolated and their magnetostructural correlations studied.[5] In most cases their formula is $[Cu_2(O_2CR)_4L_2]$ [R = alkyl or phenyl, L = H_2O, dimethylformamide (dmf), dimethyl sulfoxide (dmso) or pyridine (py)]. The isolation of mononuclear carboxylato-compounds has also confirmed the existence of uni- and bi-dentate co-ordination modes of the ligands.[6,7] The electrochemical behaviour of binuclear complexes as a means of determining reactivity differences between bi- and mono-nuclear complexes, electron transfer being an important reactivity mode for transition-metal compounds, has also drawn great interest.[8,9]

We have initiated studies on the co-ordination chemistry of the anti-inflammatory carboxylate agents tolmetin [1-methyl-5-(*p*-toluoyl)-1*H*-pyrrole-2-acetic acid (HL^1)], ibuprofen [α-methyl-4-(2-methylpropyl)benzeneacetic acid (HL^2)] and naproxen [6-methoxy-α-methylnaphthalene-2-acetic acid (HL^3)] with copper(II) ions[10] as well as of sulfonylurea drugs with transition-metal and d[10] metal ions, in an attempt to examine their mode of binding and how they affect drug delivery.[11] In this paper we report the solution behaviour of mono- and bi-nuclear copper(II) complexes with HL^1–HL^3 and the electrochemistry of these compounds in an attempt to define which complexes are dominant in different solvents and the similarities or differences in the solid state. We also report the molecular and crystal structure of the mononuclear compound $[CuL^3_2(py)_2(H_2O)]$ **1**.

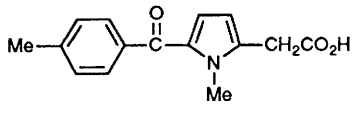

HL^1

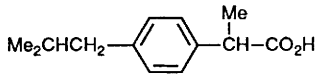

HL^2

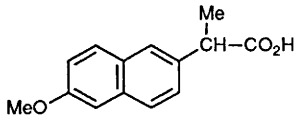

HL^3

Results and Discussion

The synthesis of the bi- and mono-nuclear complexes has been achieved *via* the reaction of $CuCl_2 \cdot 2H_2O$ with the sodium salts of the ligands. All the dimeric complexes are green crystalline

† *Supplementary data available:* see Instructions for Authors, *J. Chem. Soc., Dalton Trans.*, 1992, Issue 1, pp. xx–xxv.

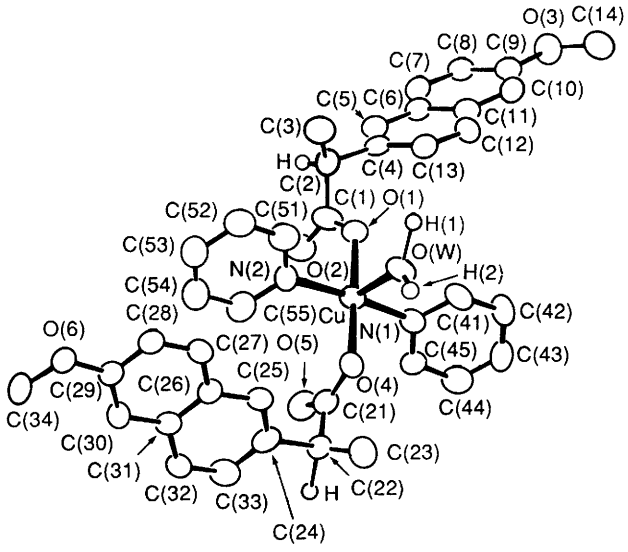

Fig. 1 An ORTEP view of the structure of $[CuL^3{}_2(py)_2(H_2O)]$ showing the atom-labelling scheme with 50% probability ellipsoids

Table 1 Summary of crystal and intensity data collection

Formula	$C_{38}H_{38}CuN_2O_7$
M	692.28
Space group	$P2_1$
a/Å	16.112(3)
b/Å	5.8692(9)
c/Å	18.130(3)
β/°	75.818(7)
U/Å^3	1662.22(8)
Z	2
D_c/Mg m^{-3}	1.395
D_m/Mg m^{-3}	1.38
μ/cm^{-1}	6.97
Scan speed/° min^{-1}	4.5
Scan range/°	$1.9 + \alpha_1 - \alpha_2$
2θ limit/°	52.0
Data collected	6784
Data unique	6537
Data used [$F_o > 8\sigma(F_o)$]	5395
R_{int}	0.022
h,k,l ranges	0 to 19, −7 to 7, −22 to 22
Weighting scheme	$1/w = \sigma^2(F_o) + 0.000\,05F_o^2$
$F(000)$	730
Refined parameters	572
$\lvert\Delta/\sigma\rvert_{max}$	0.341
Maximum, minimum Δρ/e Å^{-3}	0.924, −0.636
S[a]	4.17
R (obs.)[b]	0.0483
R (all data)[b]	0.0626
R' (obs.)[c]	0.0656
R' (all data)[c]	0.0708

[a] $S = [\Sigma w(\Delta F)^2/(N - P)]^{\frac{1}{2}}$ where P = number of parameters, N = number of observed reflections. [b] $R = \Sigma|\Delta F|/\Sigma|F_o|$. [c] $R' = [\Sigma w(\Delta F)^2/\Sigma w|F_o|^2]^{\frac{1}{2}}$.

solids soluble in dmf, dmso, py and CH_2Cl_2. The mononuclear complexes are blue crystalline solids, soluble in dmf, dmso and CH_2Cl_2. None of the complexes is an electrolyte in dmf, dmso, py or CH_2Cl_2 solutions. Crystals of $[CuL^3{}_2(py)_2(H_2O)]$ **1** suitable for X-ray analysis were obtained from py–dmso–CH_2Cl_2 (4:1:1) by standing at room temperature for about 1 week.

Description of the Structure.—In complex **1** the carboxylate group of naproxen behaves as a unidentate ligand. An ORTEP diagram of **1** is given in Fig. 1, selected bond distances and angles in Table 3. In this complex the copper atom is five-co-ordinate and could be described as having a distorted square-pyramidal geometry. The changes in bond lengths described by the tetragonality[12a] $T^5 = 0.905$ and the in-plane angular distortions[12b] described by the ratio τ (=16.33%) show the distortion away from the regular square-based pyramidal geometry. The two nitrogen atoms N(1) and N(2) (2.06 and 2.02 Å) and the carboxylato oxygen atoms O(1) and O(4) (1.93 and 1.95 Å) occupy *trans* positions in the basal plane, while the water oxygen is 2.20 Å away. The free carboxylato-oxygen atoms O(2) and O(5) lie below the basal plane of the pyramid [3.137(6) and 3.131(4) Å]. The ligand atoms which form this basal plane are not strictly coplanar. Atoms N(1) and N(2) are 0.10 and 0.06 Å below the plane and O(1) and O(4) are 0.10 and 0.08 Å above the plane, towards the apex.

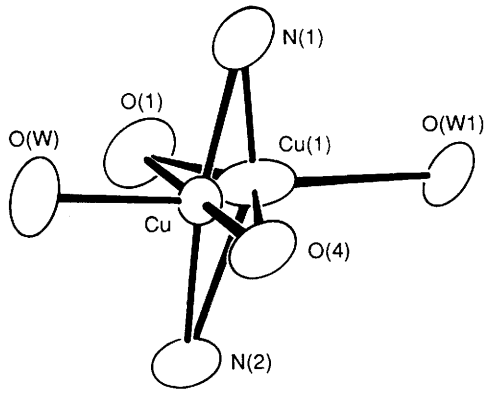

Fig. 2 An ORTEP view of the disordered Cu–O(W) group which was refined with an occupancy of 0.797, Cu(1)–O(W1) with 0.203

A feature of this structure is that Cu–O(W) group is disordered. To our knowledge this is the first crystal structure with a disordered central copper atom. A similar disorder has been observed for the compound $[PPh_4]_2[Fe(WS_4)(NO)_2]$ with occupancy factors of 0.8 and 0.2 for the Fe and W atoms.[13] The structure was refined by using a model with the Cu being assigned occupancy factors of 0.797 and 0.203, respectively. An ORTEP diagram showing the two positions of the central atom as well as the position of the two water–oxygen atoms O(W) and O(W1) is given in Fig. 2. The Cu–O(W) distance of 2.20 Å is comparable with those observed for the methoxyacetato (2.24 Å)[7b] or maleato (2.26 Å)[12c] analogues. The water molecule is hydrogen bonded to the unco-ordinated carboxylate oxygen atoms of one neighbouring molecule. Atom O(W) is 2.657(8) Å away from O(2) and 2.758(6) Å away from O(5). One of the hydrogen atoms of the water molecule bridges O(W) and O(2) and the other, O(W) and O(5).

The copper atom (Cu) is displaced 0.11 Å toward the water ligand. Considering the copper atom with 20% occupancy [Cu(1)], the displacement of this atom from the basal plane is 0.58 Å and the Cu(1)–O(W1) distance 2.59 Å.

The N–Cu–N system of the basal plane gives an angle of N(1)–Cu–N(2) 169.2(2)°, while the O–Cu–O system is almost linear [O(1)–Cu–O(4) 179.0(2)°]. The two pyridine molecules and the naphthalene group of one of the naproxen ligands are nearly coplanar, while the dihedral angle between the other naphthalene group and the pyridine plane is 73.50°.

EPR Spectra.—Samples of the mononuclear complexes in CH_2Cl_2–dmf (4:1), which have been frozen to 77 K, exhibit spectra like that shown in Fig. 3. The values of their spin-Hamiltonian parameters are not influenced by the ligands in a noticeable way. The glass spectra obtained are axial. The spectra consist of well resolved superhyperfine lines with a splitting of *ca.* 14×10^{-4} cm^{-1} characteristic of in-plane bonded nitrogen atoms. The experimental g and A parameters of the spectra are given in Table 4, and are consistent with mono-

Table 2 Positional parameters ($\times 10^4$) of the non-H atoms of $[CuL^3{}_2(py)_2(H_2O)]$

Atom	*x*	*y*	*z*	Atom	*x*	*y*	*z*
Cu	−85.6(5)	2693(2)	2679.6(4)	C(55)	984(4)	4650(9)	1233(3)
O(W)	−78(3)	−1059(7)	2681(3)	C(4)	−3147(2)	3664(7)	2672(2)
Cu(1)	−159(2)	3870(10)	2815(2)	C(5)	−3844(3)	5112(7)	2831(2)
O(W1)	−230(10)	8260(20)	2910(10)	C(6)	−4595(2)	4625(6)	3393(2)
O(1)	−1215(2)	2830(7)	2488(2)	C(7)	−5325(3)	6024(7)	3549(2)
O(2)	−1304(3)	6478(8)	2320(5)	C(8)	−6045(3)	5428(8)	4083(3)
C(1)	−1564(3)	4555(9)	2292(3)	C(9)	−6086(3)	3384(6)	4489(2)
C(2)	−2375(3)	4212(8)	2024(2)	C(10)	−5392(3)	1991(6)	4374(2)
C(3)	−2221(3)	2320(10)	1424(3)	C(11)	−4628(2)	2565(8)	3809(2)
N(1)	−646(2)	3071(7)	3825(2)	C(12)	−3898(3)	1150(7)	3656(3)
C(41)	−1162(3)	1406(8)	4171(3)	C(13)	−3200(3)	1651(8)	3106(3)
C(42)	−1484(3)	1281(8)	4932(3)	O(3)	−6857(2)	3033(6)	4997(2)
C(43)	−1267(3)	3002(9)	5384(3)	C(14)	−6970(3)	931(9)	5415(3)
C(44)	−767(3)	4701(8)	5030(3)	C(24)	2941(2)	4081(8)	2032(2)
C(45)	−466(3)	4707(8)	4268(3)	C(25)	2887(2)	2500(8)	1484(2)
O(4)	1052(2)	2609(7)	2880(2)	C(26)	3313(2)	2886(8)	708(2)
O(5)	1268(2)	6313(6)	2883(2)	C(27)	3262(3)	1340(8)	118(3)
C(21)	1496(3)	4282(8)	2888(2)	C(28)	3642(3)	1814(8)	−627(3)
C(22)	2446(3)	3768(9)	2859(2)	C(29)	4102(2)	3851(7)	−820(2)
C(23)	2616(3)	1482(9)	3193(3)	C(30)	4189(3)	5361(7)	−264(2)
N(2)	439(2)	2970(8)	1550(2)	C(31)	3785(2)	4914(7)	501(2)
C(51)	263(3)	1406(9)	1091(3)	C(32)	3845(3)	6461(8)	1091(3)
C(52)	626(4)	1380(10)	327(4)	C(33)	3441(3)	6047(8)	1818(3)
C(53)	1203(3)	3130(10)	5(3)	O(6)	4442(2)	4106(6)	−1580(2)
C(54)	1379(4)	4730(10)	464(3)	C(34)	4904(3)	6124(8)	−1832(3)

Table 3 Selected bond lengths (Å) and angles (°)

Cu–O(W)	2.202(4)	Cu(1)–O(W1)	2.59(1)
Cu–O(1)	1.935(3)	Cu(1)–O(1)	2.026(5)
Cu–N(1)	2.063(3)	Cu(1)–N(1)	1.866(5)
Cu–O(4)	1.955(3)	Cu(1)–O(4)	2.117(5)
Cu–N(2)	2.021(3)	Cu(1)–N(2)	2.320(5)
O(W)–Cu–O(1)	92.7(2)	O(W1)–Cu(1)–O(1)	107.2(5)
O(W)–Cu–N(1)	96.2(2)	O(W1)–Cu(1)–N(1)	100.6(4)
O(W)–Cu–O(4)	88.2(2)	O(W1)–Cu(1)–O(4)	111.5(4)
O(W)–Cu–N(2)	94.6(2)	O(W1)–Cu(1)–N(2)	107.0(4)
O(1)–Cu–N(1)	88.7(1)	O(1)–Cu(1)–N(1)	91.8(2)
O(1)–Cu–O(4)	179.0(2)	O(1)–Cu(1)–O(4)	139.7(2)
O(1)–Cu–N(2)	89.6(1)	O(1)–Cu(1)–N(2)	79.5(2)
N(1)–Cu–O(4)	90.9(1)	N(1)–Cu(1)–O(4)	91.7(2)
N(1)–Cu–N(2)	169.2(2)	N(1)–Cu(1)–N(2)	152.4(2)
O(4)–Cu–N(2)	90.7(1)	O(4)–Cu(1)–N(2)	79.1(2)

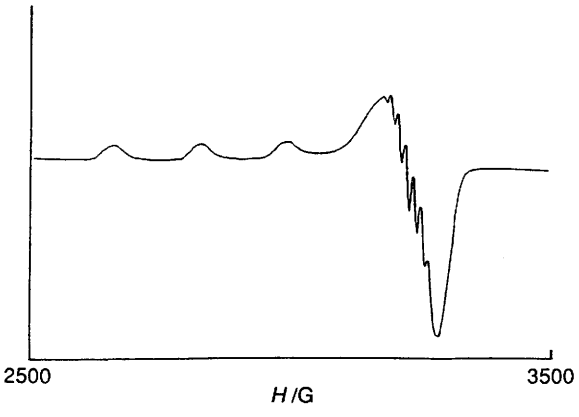

Fig. 3 X-Band EPR spectrum of $[CuL^2{}_2(py)_2(H_2O)]$ as a dmf–CH_2Cl_2 (1:4) glass at 77 K; G = 10^{-4} T

nuclear copper(II) complexes in $d_{x^2-y^2}$ ground states.[14–16] The numerical value of $G = g_{\|} - g_{\perp}/2$, indicates that exchange-coupling effects invalidate the use of the observed *g* values to support a square-pyramidal or octahedral environment in solution.[14–16] The superhyperfine splitting due to the nitrogen atoms which is consistent with a $d_{x^2-y^2}$ ground state is also consistent with a square-pyramidal or octahedral environment in solution.

Table 4 Spin-Hamiltonian parameters of the mononuclear copper(II) complexes

Compound	$g_{\|}$	$g_{\perp}$	$10^4 A_{\|}$/cm^{-1}	$10^4 A_N$/cm^{-1}	*G*
$[CuL^1{}_2(py)_2(H_2O)]$	2.290	2.050	175	13.6	5.8
$[CuL^3{}_2(py)_2(H_2O)]$	2.301	2.057	176	13.5	5.28
$[CuL^2{}_2(py)_2(H_2O)]$	2.295	2.049	176	14.3	6.02

Electronic Absorption Spectra.—The electronic spectra of all the complexes prepared have been recorded by solution techniques using dmso, dmf, CH_2Cl_2 and pyridine as solvents. In dmso and dmf both bi- and mono-nuclear complexes exhibit one broad absorption (band I) at ≈720 nm, a shoulder (band II) at ≈370 nm and a strong band (III) at ≈310 nm. The absorption coefficients given in Table 5 indicate that the mononuclear complexes are not totally converted into the dimeric form, but that a monomer ⇌ dimer equilibrium exists. The position of band I is sensitive to the nature of the axial ligand. It appears at lower energy as the donor power of the axial ligand increases. The origin of the three bands has been a topic of great discussion.[17] It is suggested that band I could be assigned to a $d_{xz,yz} \longrightarrow d_{x^2-y^2}$ transition,[18] II to a $d_{z^2} \longrightarrow d_{x^2-y^2}$ transition[18] or to a transition to a doubly excited state[19] of the type $(d_{z^2} \longrightarrow d_{x^2-y^2})^2$, without ruling out a charge-transfer assignment.[20] Band III has been assigned to a carboxylate copper(II) charge-transfer transition since no significant solvent effect on this band was observed.[21]

In CH_2Cl_2 band II is not observed for $[Cu_2L^1{}_4(dmso)_2]$ and $[Cu_2L^2{}_4(dmso)_2]$ but a dimeric form cannot be rejected because of the absence of band II.[22]

Band I also could be diagnostic for the electron-withdrawing ability of the carboxylate ligands.[20] It is shifted to lower energy with increasing electron-withdrawing ability of the ligands (Table 5) in the order $L^1 > L^3 > L^2$.

For all the pyridine complexes, the dimer or monomer

Table 5 Electronic spectra of copper(II) compounds

Compound	λ_{max} (log ε/dm^3 mol^{-1} cm^{-1}) dmso	dmf	CH_2Cl_2	py
$[Cu_2L^3{}_4(dmso)_2]$	720 (2.66)	710 (2.70)	700 (2.65)	650 (1.91)
$[CuL^3{}_2(py)_2(H_2O)]$	716 (2.48)	705 (2.48)	703 (2.46)	650 (1.93)
$[Cu_2L^1{}_4(dmso)_2]$	741 (2.59)	721 (2.60)	720 (2.63)	650 (1.80)
$[CuL^1{}_2(py)_2(H_2O)]$	745 (2.45)	722 (2.45)	719 (2.48)	650 (1.82)
$[Cu_2L^2{}_4(dmso)_2]$	707 (2.58)	700 (2.60)	690 (2.62)	653 (1.82)
$[CuL^2{}_2(py)_2(H_2O)]$	710 (2.43)	705 (2.42)	700 (2.40)	649 (1.80)

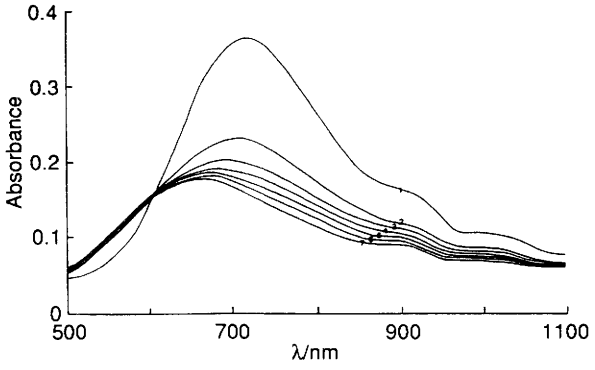

Fig. 4 Titration of $[Cu_2L^3{}_4(dmso)_2]$ with pyridine: 0.12 mmol of pyridine were added to an initial (10 cm^3) volume of the complex (9.5×10^{-3} mol dm^{-3}) in dmf (spectrum 1). The final spectrum (7) corresponds to the addition of 2.5 cm^3 (3.10 mmol) pyridine; K_1 = 5.4×10^{-6} dm^3 mol^{-1}

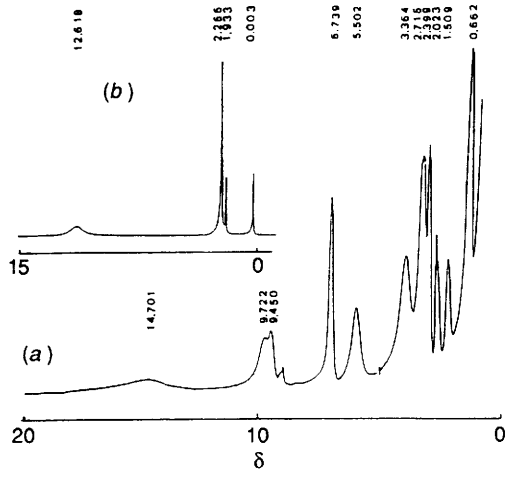

Fig. 5 Paramagnetic ^{1}H NMR spectra of (*a*) $[CuL^2{}_2(py)_2(H_2O)]$ in CD_3COCD_3 and (*b*) $[Cu_2(MeCO_2)_4(H_2O)_2]$ in CD_3CN

exhibits one broad absorption band at ≈650 nm and a strong band at ≈310 nm, indicating that in pyridine all the complexes are converted into the monomeric form. When pyridine is titrated into a solution of $[Cu_2L^3{}_2(Me_2SO)_2]$ in dmf the spectra shown in Fig. 4 are obtained. The isosbestic point at 610 nm demonstrates that $[Cu_2L^3{}_4(dmf)_2]$ and $[CuL^3{}_2(py)_2]$ are the only copper-containing species in solution.

NMR Studies.—The ^{1}H NMR spectrum obtained for $[CuL^2{}_2(py)_2(H_2O)]$ in CD_3COCD_3 is shown in Fig. 5(*a*). It contains one proton resonance that lies outside of the diamagnetic

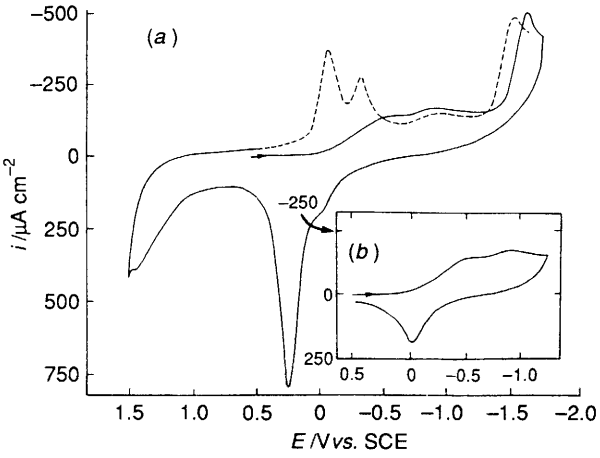

Fig. 6 Cyclic voltammograms in dmf of $[Cu_2L^3{}_4(dmso)_2]$ (*a*) in the range +1.5 to −1.7 V, (*b*) in the range +0.7 to −1.2 V. Concentration 1×10^{-3} mol dm^{-3}. Scan rate = 0.10 V s^{-1}. The supporting electrolyte was 0.1 mol dm^{-3} tetraethylammonium perchlorate

region. This broad peak is observed downfield (12–15 ppm) and has been assigned to the protons of the co-ordinated aqua group. This assignment is supported by the spectrum of $[Cu_2(MeCO_2)_4(H_2O)_2]$ which clearly shows that the broad band at δ 12.6 can be assigned to aqua protons [Fig. 5(*b*)]. It has also been confirmed by replacement of water with D_2O when the peak around δ 12–14 disappears. For all the mononuclear complexes the broad band between δ 12 and 15 is indicative that the water molecule remains co-ordinated to copper ion in solution. All the dimers give signals only in the diamagnetic region, some of them reasonably sharp, some broad.[23]

Electrochemical Studies.—The electrochemical oxidation and reduction of the bi- and mono-nuclear compounds have been studied in dmf and py solutions respectively using cyclic voltammetry at a carbon-fibre electrode.

The behaviour of $[Cu_2L^3{}_4(dmso)_2]$ is shown in Fig. 6(*a*) and is reasonably typical of all the binuclear complexes. The complete scan (+1.5 to −1.7 V) shows three cathodic processes at E_{pc} values of −0.50, −0.90 and −1.60 V, a large anodic feature at E_{pa} +0.25 V and two smaller anodic features at +0.03 and +1.40 V. The large peak at +0.25 V is characteristic of an electrochemically active species adsorbed on the electrode.[24] It was considered to be copper metal and confirmed by holding the potential at −1.70 V when a black solid was formed on the carbon-fibre surface. The presence of Cu was detected chemically. In a second scan two more reduction waves at −0.05 and −0.32 V appeared with a small shift of the reduction wave at −1.60 to −1.50 V.

Scanning in the range +0.70 to −1.20 V for $[Cu_2L^3{}_4(dmso)_2]$ gave the results shown in Fig. 6(*b*). The two one-electron waves at −0.50 and −0.90 V suggest a reduction of the binuclear species in two steps, while the oxidation occurs at −0.03 V in one step. The reduction at −0.90 V is followed by a disproportionation.[24]

The observation of an oxidation wave at +1.40 V could be assigned to a one-electron oxidation[25] of the dimer, following by decomposition. This process is consistent with the presence of Cu^{2+} ion in solution and it has been confirmed using $Cu(ClO_4)_2$ in dmf[26] [Fig. 7(*b*)]. It is also supported by the lack of the peaks, after successive scans (1–4), at −0.5 and −0.9 V which have been assigned to $[Cu^{II}Cu^{II}] \longrightarrow [Cu^{I}Cu^{II}]$ and $[Cu^{I}Cu^{II}] \longrightarrow [Cu^{I}Cu^{I}]$ reduction processes [Fig. 7(*a*)], while the peak at −0.32 V is characteristic of a $Cu^{+} \longrightarrow Cu$ process.

Considering all the above given processes, the complete pattern in the range +1.5 to −1.7 V can be described by Scheme 1.

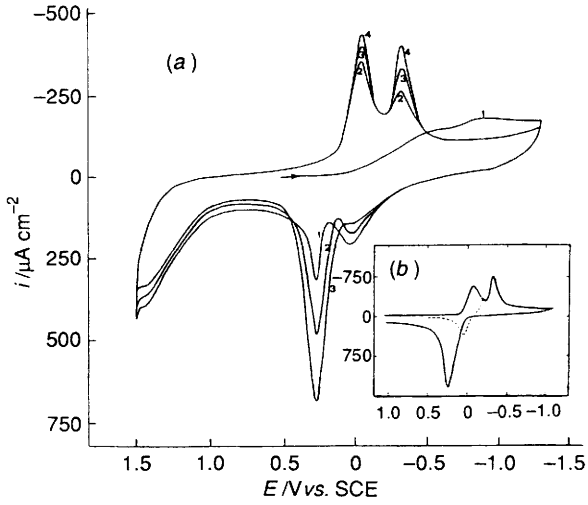

Fig. 7 Cyclic voltammograms in dmf of (*a*) $[Cu_2L^3{}_4(dmso)_2]$ in the range +1.5 to −1.3 V, (*b*) $Cu(ClO_4)_2$ in the range +0.8 to −1.0 V. Concentration 1 × 10^{-3} mol dm^{-3}. Scan rate = 0.10 V s^{-1}

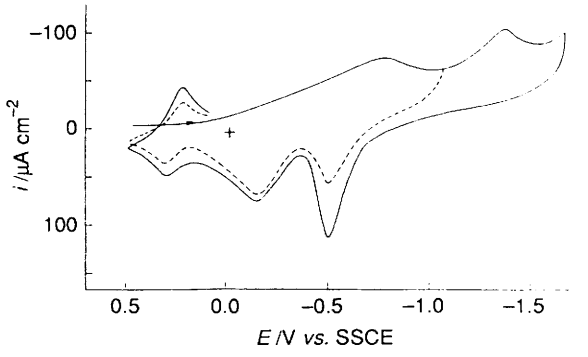

Fig. 8 Cyclic voltammograms of $[CuL^3{}_2(py)_2(H_2O)]$ in py, in the range +0.5 to −1.7 V. Concentration 1 × 10^{-3} mol dm^{-3}, scan rate = 0.10 V s^{-1}

$$[Cu^{II}Cu^{II}] + e \xrightarrow{-0.50\ V} [Cu^{I}Cu^{II}] + e \xrightarrow{-0.90\ V} [Cu^{I}Cu^{I}] + e \xrightarrow{-1.60\ V} 2Cu$$

$$2[Cu^{I}Cu^{I}] \longrightarrow [Cu^{II}Cu^{II}] + 2Cu$$

$$[Cu^{II}Cu^{II}] \xrightarrow{+1.40\ V} [Cu^{II}Cu^{II}]^{+} + e \xrightarrow{\text{decomposition}} 2Cu^{2+} + L^{+}$$

$$Cu^{2+} + e \underset{+0.03\ V}{\overset{-0.05\ V}{\rightleftharpoons}} Cu^{+} + e \xrightarrow{-0.32\ V} Cu$$

$$Cu \xrightarrow{+0.25\ V} Cu^{2+} + 2e$$

Scheme 1

For the mononuclear complex $[CuL^3{}_2(py)_2(H_2O)]$ the cyclic voltammogram in the range +0.5 to −1.7 V is shown in Fig. 8. The complete scan in this range shows two cathodic waves at −0.75 and −1.35 V and three anodic waves at −0.5, −0.15 and +0.32 V. The two one-electron waves at −0.75 and −1.35 V suggest a reduction of the mononuclear species in two steps. The reduction at −0.75 V is followed by a disproportionation.[27]

In a second scan one more reduction wave at +0.32 V is observed. This wave and the anodic wave at +0.22 V, forming a quasi-reversible couple, as well as the oxidation wave at −0.50 V are assigned to copper ion as it has been confirmed using $Cu(ClO_4)_2$ in pyridine. Finally the oxidation wave at −0.15 V can be assigned to a $[Cu^{I}] \longrightarrow [Cu^{II}]$ oxidation process of the complex.

Considering all the above given processes the complete pattern in the range +0.5 to −1.7 V can be described by Scheme 2.

$$[Cu^{II}] + e \xrightarrow{-0.75\ V} [Cu^{I}] + e \xrightarrow{-1.35\ V} Cu$$

$$[Cu^{I}] \xrightarrow{-0.15\ V} [Cu^{II}] + e$$

$$2[Cu^{I}] \longrightarrow [Cu^{II}] + Cu$$

$$Cu \xrightarrow{-0.50\ V} Cu^{+} + e \underset{+0.32\ V}{\overset{+0.22\ V}{\rightleftharpoons}} Cu^{2+} + e$$

Scheme 2

Experimental

Preparation of the Ligands.—The sodium salts of the ligands were prepared by the reaction of the protonated ligand with sodium in diethyl ether. The white solids were recrystallized from methanol and dried in the air. The binuclear complexes were prepared according to the procedure described previously.[10]

Preparation of the Mononuclear Complexes.—The sodium salt of the ligand (4 mmol) and $CuCl_2{\cdot}2H_2O$ (2 mmol) were mixed in dmso (30 cm^3). After 1 h of reflux the reaction mixture was filtered, cooled to room temperature and pyridine (30 cm^3) added. Blue crystalline products were deposited upon standing overnight. Crystals suitable for X-ray structure analysis were obtained from py–dmso–CH_2Cl_2 (4:1:1) by standing at room temperature for about 1 week.

$[CuL^3{}_2(py)_2(H_2O)]$ (Found: C, 65.10; H, 5.40; Cu, 9.20; N, 1.30. Calc.: C, 65.35; H, 5.45; Cu, 9.10; N, 4.00%): major IR absorption bands (3400–250 cm^{-1}) at 3240m, 3060w, 2960m, 2920w, 1605vs, 1450s, 1390vs, 1070s, 1025m, 860s, 705s, 420 (br), 355w and 320 cm^{-1}; ^1H NMR (CD_3CN) δ 14.90 (vbr, H_2O); (CD_3COCD_3) 14.80 (vbr, H_2O).

$[CuL^1{}_2(py)_2(H_2O)]$ (Found: C, 63.50, H, 5.40; Cu, 8.25; N, 7.40. Calc.: C, 63.85; H, 5.30; Cu, 8.45; N, 7.45%): IR (3400–250 cm^{-1}) 3240m, 3260w, 3090w, 3060w, 2920m, 1600vs, 1450m, 1370s, 1270s, 1070s, 1045m, 880s, 750m, 700s, 505m, 430 (br), 350 (br) and 320w cm^{-1}; ^1H NMR ($CDCl_3$) δ 12.71 (vbr, H_2O); (CD_3CN) 15.04 (vbr, H_2O).

$[CuL^2{}_2(py)_2(H_2O)]$ (Found: C, 66.00; H, 7.25; Cu, 9.45; N, 4.40. Calc.: C, 66.40; H, 7.05; Cu, 9.75; N, 4.30%): IR (3400–250 cm^{-1}) 3200w, 3060w, 2950m, 2920m, 2860m, 1620vs, 1595s, 1450m, 1410s, 1040s, 795s, 700s, 420 (br), 372w and 320w cm^{-1}; ^1H NMR (CD_3COCD_3) δ 14.70 (vbr, H_2O).

Physical Measurements.—The UV/VIS spectra were recorded on a Perkin Elmer–Hitachi dual-beam spectrophotomer, infrared spectra (200–4000 cm^{-1}) on a Perkin Elmer 467 spectrometer with samples prepared as KBr pellets or as Nujol mulls and solution EPR spectra on a Bruker ER200E-SRC spectrometer equipped with a Varian variable-temperature controller and diphenylpicrylhydrazyl as an external standard. Electric conductance measurements were carried out with a WTW LF 530 conductivity outfit and a type C cell which had a cell constant of 0.096. This represents a mean value calibrated at 25 °C with KCl. ^1H NMR spectra of the model complexes were obtained on a Bruker 360 MHz FT-NMR spectrometer operating in the quadrature detection mode (^1H frequency, 360.1 MHz). Spectra were collected by using a one-pulse sequence with a 90° pulse of 9.9 μs. Between 3000 and 10 000 transients were accumulated over a 50 kHz bandwidth for each sample. The spectra contained 8 K data points, and the signal-to-noise ratio was improved by apodization of the free induction decay, which introduced a negligible 10–20 Hz line broadening. Chemical shifts were referenced to $SiMe_4$ or resonances due to residual protons present in the deuteriated solvents.

Cyclic voltammetry studies were performed on a G. Bank Electronic, type Wenking PCA 72L electrochemical analyser using a three-electrode cell. The working electrode comprised carbon fibres (Celanese, Celion GY-70SE) immersed to a depth of 25 mm, which corresponds to 1 mg. A platinum wire was used as the counter electrode and a calomel electrode saturated with NaCl (SCCE) as the reference. The supporting electrolyte, tetraethylammonium perchlorate, was purchased from Carlo Erba. Prior to use it was recrystallized twice from ethanol and dried under vacuum. Oxygen was removed by purging the solutions with pure nitrogen which had been previously saturated with solvent vapour. All electrochemical measurements were performed at 25.0 ± 0.2 °C maintained by means of a thermostatically controlled water-bath.

X-Ray Crystallography.—A blue parallelepiped crystal of $[CuL^3{}_2(py)_2(H_2O)]$ with approximate dimensions 0.28 × 0.31 × 0.41 mm was mounted in a glass capillary. Complete crystal data and parameters for data collection are reported in Table 1. The space group was determined by preliminary Weissenberg and precession photographs ($0k0$, $k = 2n$). Unit-cell dimensions were derived from a least-squares refinement of the setting angles of 15 automatically centred reflections in the range $20 < 2\theta < 22°$ on a Syntex $P2_1$ diffractometer with niobium-filtered Mo-Kα radiation (λ 0.710 69 Å). Three standard reflections measured every 67 showed < 3.0% intensity fluctuation. Lorentz polarization and ψ-scan (maximum absorption correction applied 1.04) absorption corrections were applied. Scattering factors were taken from ref. 28(*a*), and the figure plotted with ORTEP.[28b]

Solution and refinement of the structure. The structure was solved by direct methods using the program SHELX 86.[29] The refinement was carried out in two blocks by full-matrix least squares, in which $\Sigma w\Delta^2$ was minimized using SHELX 76.[30] The statistics clearly indicated a non-centrosymmetric space group and the refinement proceeded in $P2_1$. The hydrogen positions except those of the methyl hydrogens were located from a difference map and were refined isotropically. The methyl hydrogen atoms were refined isotropically at calculated positions riding on their respective carbon atoms at 0.96 Å. The non-hydrogen atoms were refined anisotropically. When the refinement proceeded to $R \approx 0.08$ the Fourier difference map showed two peaks of about 6 and 1.5 e Å^{-3}, the strongest lying close to Cu. If these peaks are treated as a second disordered position for the Cu–O group, then a refinement maintaining the molecular composition suggests disorder with occupancies of 0.797 and 0.203. The hydrogen positions for the second Cu–O(W) group could not be found. The alternative model with all coordinates changed in sign refined to $R = 0.062$ and $R' = 0.856$ for observed data.

The fractional atomic coordinates of the non-H atoms are listed in Table 2, bond lengths and angles of the co-ordination sphere in Table 3.

Additional material available from the Cambridge Crystallographic Data Centre comprises H-atom coordinates, thermal parameters and remaining bond lengths and angles.

Acknowledgements

We thank Professor D. A. Jannakoudakis for his useful suggestions in the course of the electrochemical study, and the University of Michigan, Department of Chemistry for use of facilities.

References

1 J. R. J. Sorenson, in *Metal Ions in Biological Systems*, ed. H. Sigel, Marcel Dekker, New York, 1982, vol. 14, p. 77.
2 J. R. J. Sorenson, V. Kishore, A. Pezeshk, L. W. Oberley, S. W. C. Leuthauser and T. D. Oberley, *Inorg. Chim. Acta*, 1984, **91**, 285; V. Weser, K.-H. Sellinger, E. Lengfelder, W. Werner and J. Strahle, *Biochim. Biophys. Acta*, 1980, **631**, 232.
3 G. N. La Mar, G. R. Eaton, R. H. Holm and F. A. Walker, *J. Am. Chem. Soc.*, 1973, **95**, 63 and refs. therein.
4 P. Kourounakis, *Handbook of Pharmaceutical Chemistry*, 2nd edn., Thessaloniki, 1987 (in Greek).
5 R. J. Doedens, *Prog. Inorg. Chem.*, 1975, **19**, 173; M. Melnik, *Coord. Chem. Rev.*, 1982, **42**, 259; M. Kato and Y. Muto, *Coord. Chem. Rev.*, 1988, **92**, 45.
6 C. K. Prout, M. J. Barrow and F. J. C. Rossoti, *J. Chem. Soc. A*, 1971, 3326; C. K. Prout, R. A. Armstrong, J. R. Carruthers, J. G. Forrest, P. Murray Rust and F. J. C. Rossoti, *J. Chem. Soc. A*, 1968, 2791.
7 G. Davey and F. S. Stephens, *J. Chem. Soc. A*, 1971, (*a*) 1917; (*b*) 2577.
8 J. P. Gisselbrecht, M. Gross, A. H. Alberts and J. M. Lehn, *Inorg. Chem.*, 1980, **19**, 1386; R. L. Lintvedt and L. S. Kramer, *Inorg. Chem.*, 1983, **22**, 796; R. L. Lintvedt, G. Ranger and B. A. Schoenfelner, *Inorg. Chem.*, 1984, **23**, 688; R. L. Lintvedt, B. A. Schoenfelner and K. A. Rupp, *Inorg. Chem.*, 1986, **25**, 688; J. K. Zehetmair and R. L. Lintvedt, *Inorg. Chem.*, 1990, **29**, 2201; D. E. Fenton and R. L. Lintvedt, *J. Am. Chem. Soc.*, 1978, **100**, 636; D. E. Fenton, R. P. Schroeder and R. L. Lintvedt, *J. Am. Chem. Soc.*, 1978, **100**, 1931; R. C. Long and D. N. Hendrickson, *J. Am. Chem. Soc.*, 1983, **105**, 1513; R. R. Gagne, C. A. Koval, J. Smith and M. C. Cimolino, *J. Am. Chem. Soc.*, 1979, **101**, 4571; R. Bradbury, J. L. Hampton, D. P. Martone and A. W. Maverick, *Inorg. Chem.*, 1989, **28**, 2392; E. J. Laskowski, D. M. Duggan and D. N. Hendrickson, *Inorg. Chem.*, 1975, **14**, 2449; H. Doine, F. F. Stephens and R. D. Cannon, *Inorg. Chim. Acta*, 1983, **75**, 155.
9 M. F. Cabral, J. DeO Cabral, J. Van Rijn and J. Reedijk, *Inorg. Chim. Acta*, 1984, **87**, 87.
10 C. Dendrinou-Samara, D. P. Kessissoglou, G. E. Manoussakis, D. Mentzafos and A. Terzis, *J. Chem. Soc., Dalton Trans.*, 1990, 959.
11 D. P. Kessissoglou, G. E. Manoussakis, A. G. Hatzidimitriou and M. G. Kanatzidis, *Inorg. Chem.*, 1987, **26**, 1395; A. G. Hatzidimitriou, G. E. Manoussakis, D. P. Kessissoglou, P. N. Kourounakis and G. Economidis, *J. Inorg. Biochem.*, 1990, **39**, 263.
12 B. J. Hathaway, *Struct. Bonding (Berlin)*, 1973, **14**, 49; A. W. Addison, T. Nagasewar, J. Reedijk, J. van Rijn and G. C. Verchoor, *J. Chem. Soc., Dalton Trans.*, 1984, 1349; C. K. Prout, R. A. Carruthers and F. J. C. Rossoti, *J. Chem. Soc. A*, 1971, 3342.
13 A. Mueller, P. Stolz, H. Boegge, S. Satkar, K. Schmitz, A. Fangmeier, H. Bueker and W. Twistel, *Z. Anorg. Allg. Chem.*, 1988, **559**, 57.
14 I. Bertini, D. Gatteschi and A. Scozzafara, *Coord. Chem. Rev.*, 1979, **29**, 67; B. J. Hathaway and D. E. Billing, *Coord. Chem. Rev.*, 1970, **5**, 143; B. J. Hathaway, *Struct. Bonding (Berlin)*, 1984, **57**, 55.
15 I. M. Procter, B. J. Hathaway and P. Nichollis, *J. Chem. Soc. A*, 1968, 1678.
16 A. A. G. Tomlinson and B. J. Hathaway, *J. Chem. Soc. A*, 1968, 1685.
17 J. Gatterick and P. Thornton, *Adv. Inorg. Chem. Radiochem.*, 1977, **20**, 291.
18 G. W. Reimann, G. F. Kokoszka and G. Gordon, *Inorg. Chem.*, 1965, **4**, 1082.
19 A. E. Hansen and C. J. Ballhausen, *Trans. Faraday Soc.*, 1965, **61**, 631.
20 L. Dubicki and R. L. Martin, *Inorg. Chem.*, 1966, **5**, 2203.
21 D. P. Graddon, *J. Inorg. Nucl. Chem.*, 1961, **17**, 221.
22 R. Tsuchida, S. Yamada and H. Nakamura, *Nature (London)*, 1956, **178**, 1192; R. Tsuchida, S. Yamada and H. Nakam, *Nature (London)*, 1958, **181**, 479; R. Tsuchida and S. Yamada, *Nature (London)*, 1958, **182**, 1230.
23 A. Kawamori, *J. Phys. Soc. Jpn.*, 1966, **21**, 1096; M. Inoue and M. Kubo, *Inorg. Chem.*, 1970, **9**, 2310; R. A. Zelonka and M. C. Baird, *Inorg. Chem.*, 1972, **11**, 134; I. Bertini, A. Dei and A. Scozzafava, *Inorg. Chem.*, 1975, **14**, 1526.
24 G. Christou, S. P. Perlepes, E. Libby, K. Folting, J. C. Huffman, R. J. Webb and D. N. Hendrickson, *Inorg. Chem.*, 1990, **29**, 3657.
25 A. R. Hendrickson, R. L. Martin and N. M. Rohd, *Inorg. Chem.*, 1976, **15**, 2115.
26 C. Tsiamis, S. Cambanis, A. D. Jannakoudakis and E. Theodoridou, *J. Electroanal. Chem. Interfacial Electrochem.*, 1988, **252**, 109.
27 L. Ciavatta, D. Ferri and R. Palombari, *J. Inorg. Nucl. Chem.*, 1980, **42**, 593.
28 (*a*) *International Tables for X-Ray Crystallography*, eds. J. A. Ibers and W. C. Hamilton, Kynoch Press, Birmingham, 1974, vol. 4; (*b*) C. K. Johnson, ORTEP II, report ORNL-5138, Oak Ridge National Laboratory, TN, 1976.
29 G. M. Sheldrick, SHELX 86, University of Göttingen, 1986.
30 G. M. Sheldrick, SHELX 76, Program for Crystal Structure Determination, University of Cambridge, 1976.

Received 2nd *July* 1992; *Paper* 2/03503K